# Autophagy inhibition enhances isorhamnetin-induced mitochondria-dependent apoptosis in non-small cell lung cancer cells

YUSHU RUAN[1], KE HU[1] and HONGBO CHEN[2]

[1]Division of Respiratory Disease, Renmin Hospital of Wuhan University, Wuhan, Hubei 430060;
[2]The Shenzhen Key Lab of Gene and Antibody Therapy, Division of Life and Health Sciences, Shenzhen Graduate School of Tsinghua University, Shenzhen, Guangdong 518055, P.R. China

Received April 2, 2015; Accepted June 22, 2015

DOI: 10.3892/mmr.2015.4148

**Abstract.** Isorhamnetin (ISO) is a flavonoid from plants of the *Polygonaceae* family and is also an immediate metabolite of quercetin in mammals. To date, the anti-tumor effects of ISO and the underlying mechanisms have not been elucidated in lung cancer cells. The present study investigated the inhibitory effects of ISO on the growth of human lung cancer A549 cells. Treatment of the lung cancer cells with ISO significantly suppressed cell proliferation and colony formation. ISO treatment also resulted in a significant increase in apoptotic cell death of A549 cells in a time- and dose-dependent manner. Further investigation showed that the apoptosis proceeded via the mitochondria-dependent pathway as indicated by alteration of the mitochondrial membrane potential, the release of cytochrome *C* and caspase activation. Of note, treatment with ISO also induced the formation of autophagosomes and light chain 3-II protein in A549 cells. Furthermore, co-treatment with autophagy inhibitors 3-methyladenine and hydroxychloroquine significantly inhibited the ISO-induced autophagy and enhanced the ISO-induced apoptotic cell death *in vitro* as well as *in vivo*. Thus, the results of the present study suggested that ISO is a potential anti-lung cancer agent. In addition, the results indicated that the inhibition of autophagy may be a useful strategy for enhancing the chemotherapeutic effect of ISO on lung cancer cells.

## Introduction

Lung cancer is the main cause of cancer-associated mortalities worldwide. Clinically, lung cancer is divided into small cell lung cancer (SCLC) and non-SCLC (NSCLC), and NSCLC accounts for ~85% of all lung cancers (1). To date, despite multimodality treatments consisting of extended surgical resection, radiotherapy and chemotherapy, NSCLC only has a five-year survival rate of <20% (2). Hence, it is important and urgent to develop novel effective agents and approaches to treat NSCLC.

Flavonoids are a group of natural non-essential compounds that are abundantly present in fruits, vegetables, tea, seeds, nuts and red wine. Numerous flavonoid agents have been used to treat human cancers (3). Quercetin is a plant-derived bioflavonoid that exhibits several biological functions *in vitro* and *in vivo*, including anti-inflammatory, anti-oxidative and anti-cancer effects (4). A recent study has shown that an immediate 3'-*O*-methylated metabolite of quercetin, named isorhamnetin, exerts a greater anti-tumor effect as compared with that of quercetin in human colon cancer cells (5). The anti-tumor effects of ISO been investigated in a number of cancer types, including colorectal, skin and gastric cancers (6-8). However, to the best of our knowledge, the anti-cancer effect of ISO has not been investigated in lung cancer. Thus, the present study investigated the anti-proliferative and pro-apoptotic effects of ISO on the growth of human NSCLC cells.

Apoptosis, or programmed cell death, is a multi-step process that is important in controlling the cell number and proliferation as part of normal development; however, in cancer cells, cell cycle checkpoints and the subsequent progression of apoptosis are frequently inactivated. Consequently, the induction of apoptosis has been emphasized in anti-cancer strategies (9,10). Regarding the initiation and execution of cell death, two apoptotic pathways have been identified: The extrinsic (Fas death receptor-mediated) and intrinsic (mitochondrial) pathways. Either of the two pathways involves the activation of caspases (11,12). Autophagy is the primary mechanism to clear the cell from toxic proteins and damaged organelles (13,14). However, autophagy has been found to be associated with tumorigenesis and tumor progression. Autophagy can act as a potential tumor suppression factor by removing damaged organelles/proteins, suppressing cell growth and avoiding genomic instability in normal cells (15,16). However, when tumorigenesis occurs, cancer cells can utilize autophagy to confer stress tolerance, including an acidic environment, hypoxia and nutrition deficiency, which serves to promote tumor cell survival (17). In fact, a number of existing chemotherapeutic drugs designed to kill cancer cells by inducing apoptosis are most likely to also induce

*Correspondence to:* Mr. Ke Hu, Division of Respiratory Disease, Renmin Hospital of Wuhan University, 99 Zhangzhidong Road, Wuhan, Hubei 430060, P.R. China
E-mail: hukewuhan@163.com

*Key words:* isorhamnetin, apoptosis, caspase, 3-methyladenine, autophagy, lung cancer

autophagy (18). Drug-activated autophagy in cancer cells, in turn, causes resistance of the cells to death and decreases the curative effects (19). In fact, inhibition of autophagy has been shown to enhance the anti-tumor effect of diverse chemotherapeutic drugs (20-22).

In the present study, the effects of ISO on autophagy in A549 cells was investigated. For this, the effect of the inhibition of autophagy on ISO-mediated cytotoxicity and apoptosis was investigated. Furthermore, the effects of ISO on lung cancer cells were demonstrated *in vivo*. To the best of our knowledge, the present study was the first to report the effects of ISO on human lung cancer cells.

## Materials and methods

*Cell lines and reagents*. The NSCLC cell line A549 was obtained from the Chinese Type Culture Collection Center (Wuhan, China), were cultured in Dulbecco's modified Eagle's medium (DMEM; Invitrogen Life Technologies, Carlsbad, CA, USA) with 10% fetal calf serum (FCS; Invitrogen Life Technologies). Enhanced green fluorescent protein (EGFP)-light chain 3 (LC3) plasmid was kindly provided by Professor Marja Jäättelä (Cell Death and Metabolism Research Unit, Danish Cancer Society Research Center, Copenhagen, Denmark). Transfection reagent Lipofectamine 2000 was purchased from Invitrogen Life Technologies. The fluorescein isothiocyanate (FITC) Annexin V and propidium iodide (PI) kit for apoptosis detection was purchased from Invitrogen Life Technologies. The JC-1 kit for the mitochondrial membrane assay was from Beyotime Institute of Biotechnology (Haimen, China). ISO, chloroquine (CQ), 3-methyladenine (3-MA) and monodansylcadaverine (MDC) were purchased from Sigma-Aldrich (St. Louis, MO, USA). The following antibodies were used in the present study: Rabbit anti-human/mouse/rat caspase 3 polyclonal antibody (cat no. GTX110543); rabbit anti-human caspase 3 (cleaved Asp175) polyclonal antibody (cat no. GTX86909); rabbit anti-human/mouse/rat pro-caspase 9 polyclonal antibody (cat no. GTX61008); rabbit anti-human/mouse PARP polyclonal antibody (cat no. GTX100573); rabbit anti-human beta actin polyclonal antibody (cat no. GTX109639); rabbit anti-human/rat/mouse cytochrome C polyclonal antibody (cat no. GTX108585) (all from Genetex, Irvine, CA, USA). LC3 antibodies (cat. no. 2775) were from Cell Signaling Technology (Beverly, MA, USA). Beclin1 and PCNA (cat. no. sc-53407) antibodies were from Santa Cruz Biotechnology, Inc. (Dallas, TX, USA). Secondary antibodies (anti-rabbit and anti-mouse HRP-conjugated) were purchased from Keygen Biotech (Nanjing, China).

*MTT assay*. An MTT assay was used to determine the cell viability. Briefly, $1x10^4$ A549 cells/well in a 96-well plate were treated with various concentrations of ISO (0-16 $\mu$M) in the presence or absence of autophagy inhibitors (10 mM 3-MA or 50 $\mu$M CQ). At the appropriate time-points, 20 $\mu$l MTT [Sangon Biotech, Shanghai, China; 5 mg/ml in phosphate-buffered saline (PBS)] was added for 4 h at 37˚C and then all liquid was carefully removed. Optical density (OD) values were measured with a spectrophotometer (DU-7400; Beckmann-Coulter, Brea, CA, USA) at 490 nm following continuous agitation for 15 min with 100 $\mu$l dimethyl sulfoxide (DMSO; Sigma-Aldrich). The inhibitory rate was calculated according to the following formula: Inhibitory rate (%) = [1-(OD of the experimental samples/OD of the control)] x100%.

*Colony formation assay*. A549 cells were seeded in triplicate into a six-well plate ($1x10^4$ cells/well) and cultured in DMEM with 2.5% bovine serum albumin (Sigma-Aldrich) in the presence or absence of ISO (2-8 $\mu$M). After 10 days, the resulting colonies were stained with 0.05% of crystal violet (Sangon Biotech) and images were captured.

*Annexin V-fluorescein isothiocyanate/PI apoptosis assay*. A549 cells were treated with various concentrations of ISO (0-16 $\mu$M) in the absence or presence of 10 mM 3-MA or 50 $\mu$M CQ for 24 h, and then single-cell suspensions were prepared using EDTA-free trypsin (Sangon Biotech) digestion. Cells were stained according to the instruction manual of the FITC-Annexin V and PI kit and analyzed using flow cytometry (FACS Influx SE, BD Biosciences, Franklin Lakes, NJ, USA).

*DNA fragmentation assay*. A549 cells were cultured in the presence or absence of 16 $\mu$M ISO for various durations (0, 6, 12, 24, 48 or 72 h). Cells were then collected and washed with PBS. The pellet was homogenized in 450 $\mu$l lysis buffer (20 Mm Tris-HCl, pH 8.0, 10 mM EDTA, pH 8.0, 0.2% Triton X-100; Sangon Biotech) by pipetting through a blue pipette nozzle and incubated for 10 min on ice. The lysates were centrifuged for 15 min at 13,000 x g and the supernatants were incubated at 50˚C overnight with proteinase K (2 mg/ml; Sangon Biotech). DNA was precipitated with two volumes of 100% ethanol and 0.1 volumes of 3 M sodium acetate for 2 h at 70˚C. DNA was pelleted at 12,000 x g for 15 min and washed twice with 70% ethanol. DNA was dissolved in distilled water containing 1 mg/ml RNase A (Sangon Biotech), incubated for 30 min at 37˚C, and analyzed by electrophoresis on 1.5% agarose gels (Sangon Biotech) and staining with ethidium bromide (Sangon Biotech).

*Cell cycle analysis*. In order to assess whether the apoptotic effects of ISO were dependent on caspases, A549 cells were incubated with caspase-9 inhibitor Z-LEHD-FMK (BioVision, San Francisco, CA, USA) or caspase-3/7 inhibitor Z-DEVD-FMK (R&D Systems, Minneapolis, MN, USA) for 2 h followed by treatment of the cells with ISO for 48 h and subsequent flow cytometric cell cycle analysis. Following the above treatments, cells were harvested and washed in PBS. Cells were fixed in 1 ml cold 70% ethanol for 30 min on ice. Cells were pelleted at by centrifugation at high speed and the supernatant was discarded. Following two washes with PBS, the cells were incubated with 50 $\mu$l RNAse A solution to remove any RNA. Subsequently, 400 $\mu$l PI solution per $1x10^6$ cells was added and mixed. Cells were incubated for 10 min at room temperature and subjected to flow cytometric analysis (FACS Influx SE), for which at least 10,000 events were observed.

*Measurement of mitochondrial membrane potential*. The mitochondrial membrane potential was assessed using the

JC-1 assay. A549 cells were treated with 16 $\mu$M ISO for 24 h. Subsequently, 1X JC-1 suspension was added to treat the cells for 15 min at 37˚C and images of the cells were captured using confocal microscopy (FV100; Olympus, Tokyo, Japan). In healthy cells with high mitochondrial membrane potential, JC-1 is present as J-aggregate complexes with red fluorescence, while in apoptotic or unhealthy cells with reduced mitochondrial membrane potential, JC-1 remains in the monomeric form, which is characterized by green fluorescence. Furthermore, the mitochondrial membrane potential was assessed using the tetramethylrhodamine ethyl ester (TMRE) assay. For this, A549 cells were treated with ISO (8 $\mu$M) for 12, 24 or 48 h. The cells were then washed with cold PBS and stained by adding 200 nM TMRE (Sangon Biotech), a fluorescent potential-dependent indicator, followed by incubation for 30 min at 37˚C. JC-1 staining was observed by fluorescence microscopy (Ti-E; Nikon Corporation, Tokyo, Japan) and the mitochondrial membrane potential was detected by flow cytometry (FACS Influx SE) at 582 nm.

*Reverse transcription quantitative polymerase chain reaction (RT-qPCR).* Total RNA was extracted with TRIzol (Invitrogen Life Technologies) following the manufacturer's instructions. First-strand cDNA was prepared by reverse transcription with Superscript II reverse transcriptase (Invitrogen Life Technologies) and oligo(dT) primers and stored at 20˚C. Real-Time polymerase chain reaction (Real-Time PCR) was performed using SYBR® Premix Ex Taq™ II (Takara Bio Inc., Shiga, Japan) on an ABI 7300 QPCR system (Applied Biosystems, Thermo Fisher Scientific, Waltham, MA, USA). The PCR cycling conditions were as follows: 95˚C for 5 min, followed by 95˚C for 5 sec and 60˚C for 34 sec for 39 cycles. As an internal control, levels of GAPDH were quantified in parallel with target genes. Normalization and fold changes were calculated using the ΔΔCt method (23). Primers (Beijing Genomics Institute, Beijing, China) for detection of gene expression were as follows: GAPDH forward, 5'-TGGGGTGAGGCCGGTGCTGA-3' and reverse, 5'-GGCATCGGCAGAAGGGGCGG-3'; caspase-3 forward, 5'-CAGAGCTGGACTGCGGTATTGA-3' and reverse, 5'-AGCATGGCGCAAAGTGACTG-3'; caspase-8 forward, 5'-CTGGGAAGGATCGACGATTA-3' and reverse, 5'-CATGTCCTGCATTTTGATGG-3'; caspase-9 forward, 5'-AGCCAGATGCTGTCCCATAC-3' and reverse, 5'-CAGGAGACAAAACCTGGGAA-3'; B-cell lymphoma 2 (Bcl-2)-associated X protein (Bax) forward, 5'-AGACAGGGGCCTTTTTGCTAC-3', and reverse, 5'-AATTCGCCGGAGACACTCG-3'; Bcl-2 forward, 5'-CATGCTGGGAGCGTCACAT-3' and reverse, 5'-CTCCACTGAACTCGTACAAACTT-3'; Bcl-2-like protein 2 (Bclw) forward, 5'-GGTGACCTACCTGGAGACACG-3' and reverse, 5'-GTCCTCACTGATGCCCAGTTC-3'; myeloid cell leukemia 1 (Mcl-1) forward, 5'-GAAACAGCATGAGGTGTGGTA' and reverse, 5'-AGCCGAAGTTAAAACCTGTCC-3'; BH3 interacting-domain death agonist (Bid) forward, 5'-GTGATGTCAGATATGGGCAGAG-3' and reverse, 5'-ATCCCACGGATGGATAGGTCG-3'; Bcl-2/adenovirus E1B 19 kDa protein-interacting protein 3 (Bnip3) forward, 5'-GGTCCAGTAGACCCGAAAACA-3' and reverse, 5'-TGTGCTCAGTCGCTTTCCAAT-3'; Bcl-2 homologous antagonist/killer (BAK) forward, 5'-CATCAACCGACGCTATGACTC-3' and reverse, 5'-GTCAGGCCATGCTGGTAGAC-3'; P53 forward, 5'-ACAAGGTTGATGTGACCTGGA-3' and reverse, 5'-TGTAGACTCGTGAATTTCGCC-3'; P21 forward, 5'-TGCTGAATCTACGCAACCGAT-3' and reverse, 5'-TCCAGTGGCGAATCATCTACAT-3'; and p53-upregulated modulator of apoptosis (Puma) forward, 5'-GACCTCAACGCACAGTACGAG' and reverse, 5'-AGGAGTCCCATGATGAGATTGT-3'.

*Western blot analysis.* Cells were washed twice with PBS and lysed with lysis buffer. The concentration of the protein was determined by ultraviolet spectrophotometry (Ruili Analysis Instruments, Beijing, China). Equal amounts (10 $\mu$g) of protein were separated by 10% SDS-PAGE and transferred onto a polyvinylidene difluoride membrane (Sangon Biotech). The membrane was blocked with 5% non-fat milk in Tris-buffered saline containing Tween 20 (TBST; Sangon Biotech) for 2 h at room temperature and incubated overnight at 4˚C with specific primary antibodies. After washing three times with TBST, the membrane was incubated with appropriate horseradish peroxidase-linked secondary antibody for 4 h at room temperature and then detected with an enhanced chemiluminescence detection kit (Sangon Biotech) in the dark.

*Autophagy assay using pEGFP-LC3.* A549 cells seeded in six-well plates containing glass coverslips and transfected with pEGFP-LC3 plasmid for 24 h. Cells were either left untreated or pre-treated with autophagy inhibitors (10 mM 3-MA or 50 $\mu$M CQ) for 1 h. An appropriate concentration of ISO was added for an additional 24h and the cells were then fixed in 4% paraformaldehyde. EGFP-LC3-II punctate dots were detected and counted using confocal microscopy as described previously (24).

*Observation of autophagic vacuoles by MDC staining.* MDC has recently been reported as another specific marker for autophagic vacuoles (25). In the present study, MDC was therefore used to detect autophagy. A549 cells were treated with ISO as described above for 24 h and 0.05 mM MDC was then added to medium for an additional 2 h at 37˚C. Accumulation of MDC in autophagy-associated vacuoles was determined using confocal microscopy.

*Cytochrome C immunoblotting.* The cytosolic fraction was prepared as described previously (26). A549 cells treated with ISO were collected and washed with cold PBS. Cell pellets were lysed in 40 ml lysis buffer [20 mM 4-(2-hydroxyethyl)-1-piperazineethanesulfonic acid/NaOH, pH 7.5, 250 mM sucrose, 10 mM KCl, 2 mM $MgCl_2$, 1 mM EDTA, 1 mM dithiothreitol, protease inhibitor cocktail] for 20 min on ice. They were homogenized by passing the lysate through a 22-gauge needle 10 times. The homogenate was centrifuged at 25,000 x g for 30 min at 4˚C and protein contents in the supernatant were measured using a Bio-Rad DC Protein Assay kit II (Bio-Rad Laboratories, Inc., Hercules, CA, USA). The lysates containing 25 mg of protein were analyzed by western blotting for cytochrome *C* (1:2,000 dilution).

*A549 tumor model.* The study was approved by the ethics committee of the People's Hospital of Wuhan University

(Wuhan, China). BALB/c nu/nu mice (five weeks old) were purchased from Guangdong Medical Laboratory Animal Center (Guangzhou, China). Mice were housed in a specific-pathogen-free environment maintained at 25±1˚C with 55% relative humidity and given food and water *ad libitum*. A549 cells in sub-confluent condition were harvested and re-suspended in sterile PBS. A549 cells ($6x10^5$ in 200 $\mu$l PBS) were sub-cutaneously injected into the right flank of the BALB/c nu/nu mice. Four days after tumor inoculation, mice were given a daily intraperitoneal injection of ISO (0.5 mg/kg), and a percentage of the animals was co-injected with 3-MA (22.4 mg/kg) or CQ (10 mg/kg) (27); each experimental group contained six mice. Tumor volumes were measured every three days with a caliper and calculated according to the formula $V=1/2(L \times W^2)$, where L and W stand for length and width, respectively. All mice were sacrificed 13 days after tumor inoculation by $CO_2$ inhalation following anesthesia by isofluorane inhalation and the tumors were excised and weighed.

*Immunohistochemistry*. Tumor specimens were immediately removed from sacrificed mice and prepared for histological examination. Tumors were fixed in 4% neutral buffered formalin overnight, embedded in paraffin and sectioned to 6 $\mu$m thickness. The tumor sections were immobilized and de-paraffinized by immersing in xylene, dehydrated in a graded series of ethanol and washed with distilled water. For antigen retrieval, the tumor sections were boiled in 10 mM sodium citrate buffer (pH 6.0) for 10 min and cooled to room temperature. After washing with Tris-buffered saline (TBS), endogenous peroxidase activity was blocked by incubation in 3% $H_2O_2$-methanol for 10 min at room temperature. The sections were stained with antibodies against proliferating cell nuclear antigen (PCNA; Santa Cruz Biotechnology, Inc.) and caspase-3 overnight at 4˚C using Avidin-Biotin Complex and Diaminobenzidine kits (Vector Laboratories, Inc., Burlingame, CA, USA) and also counterstained with Mayer's hematoxylin solution (Sigma-Aldrich). Terminal deoxynucleotidyl transferase-mediated dUTP nick end labeling (TUNEL) staining was performed using a TACS® TdT kits (R&D Systems, Minneapolis, MN, USA) and counterstained with methyl green (Sangon Biotech). Images of all stained sections were captured using an Axiovert S 100 light microscope (Carl Zeiss, Inc., Oberkochen, Germany) at 400x magnification. At least four tumors were analyzed per group, and at least four fields of view each of at least six slices of each tumor were analyzed. Quantitative evaluation of the images was performed using PixeLink Capture OEM (Ottawa, ON, Canada) software and indexes were calculated as follows: Proliferative index (%) = (Number of PCNA positive cells/total cells) x100, Apoptotic index (%) = (Number of TUNEL-positive cells/total cells) x100, and cleaved caspase-3 index: (Number of caspase-3 positive cells/total cells) x100.

*Statistical analysis*. Values are expressed as the mean ± standard deviation of three independent experiments. Comparisons were performed using a two-tailed paired Student's t-test. GraphPad Prism version 5.01 (GraphPad Software, Inc., La Jolla, CA, USA) was used to conduct statistical analysis. $P<0.05$ was considered to indicate statistically significant differences, which was denoted in figures as $^{*}P<0.05$, $^{**}P<0.01$ and $^{***}P<0.001$.

## Results

*ISO inhibits proliferation and induces apoptosis of NSCLC cells*. To investigate the proliferation inhibition effect of ISO, an MTT assay was performed. As shown in Fig. 1A, ISO treatment significantly inhibited the proliferation of A549 cells in a dose- and time-dependent manner. In addition, ISO also significantly suppressed the colony formation ability of A549 cells in a dose-dependent manner (Fig. 1B).

In addition, to determine whether the growth inhibition is accompanied by an induction of apoptosis in A549 cells, apoptotic DNA fragmentation was assessed by gel electrophoresis. As shown in Fig. 1C, a ladder pattern of discontinuous DNA fragments was detected at 24 h after exposure to ISO, and the extent of DNA fragmentation was significantly elevated at 72 h. Similarly, a TUNEL assay also showed a significant increase in the number of apoptotic bodies following treatment with ISO (Fig. 1D). Furthermore, apoptosis was assessed using Annexin V/PI staining and flow cytometric analysis. As expected, ISO treatment resulted in a significant increase in the number of apoptotic cells with Annexin V-positive staining in a dose-dependent manner (Fig. 1E). All of these results demonstrated that ISO treatment significantly suppressed cell proliferation and colony formation, and induced apoptotic cell death in NSCLC cells in a time- and dose-dependent manner.

*ISO induces mitochondria-dependent caspase activation*. With regard to apoptosis signaling, mitochondria are a central sensor and integration point for diverse apoptotic signals; furthermore, they function as the storehouse of cytochrome *C* and Smac/Diablo, which binds and disables inhibitors of apoptosis-associated proteins (IAPs) (28,29). The 'apoptosome' cascade or intrinsic pathway involves activation of pro-caspase-9 by cytochrome C released from the mitochondria, leading to the activation of the executioner pro-caspases (caspase-3, -6 and -7) that cleave poly (adenosine diphosphate ribose) polymerase (PARP) and other apoptotic protein substrates (30). To investigate whether ISO-induced apoptosis was mitochondrial-dependent, mitochondrial membrane potential and caspase assays were performed. The permeabilization of mitochondria is one of the most important events during apoptosis (31,32). Mitochondrial de-polarization in apoptotic cells can be detected by a decrease in the red/green fluorescence intensity ratio of the dye JC-1 as a result of its disaggregation into monomers. As shown in Fig. 2A, a significantly higher red/green fluorescence rate was observed in cells treated with DMSO only compared with that in ISO-treated cells, suggesting that ISO treatment resulted in the de-polarization and permeabilization of mitochondria of A549 cells. To further verify the depolarization of the mitochondrial membrane potential after ISO treatment (16 $\mu$M), A549 cells were stained with TMRE followed by flow cytometric analysis at the indicated times. As shown in Fig. 2B, ISO treatment resulted in a left-shift of the TMRE fluorescence at as early as 12 h of incubation with ISO. The ratio of cells with intact mitochondrial membrane potential decreased from 90.2% in

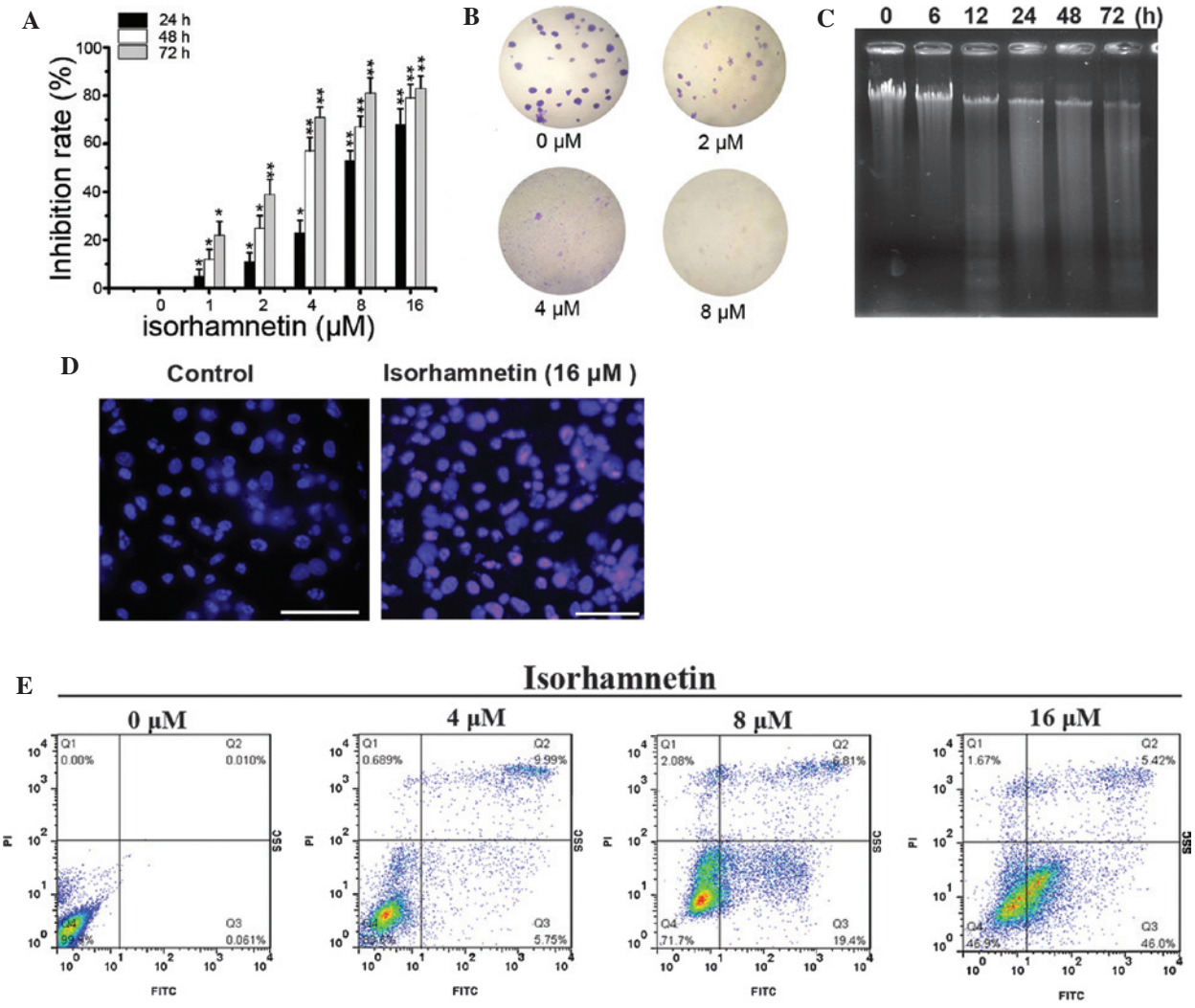


Figure 1. Effects of ISO on the viability and colony formation of A549 cells. (A) MTT cell viability assay. Values are expressed as the mean ± standard deviation of three independent experiments performed in duplicate. $^{*}$P<0.05; $^{**}$P<0.01, as compared with 0 $\mu$M isorhamnetin. (B) Colony formation assay. A549 cells were treated with indicated concentrations of ISO for 72 h and cell colonies were visualized by crystal violet staining (magnification, x40). (C) Apoptotic DNA fragmentation was detected by agarose gel electrophoresis at the indicated time-points after exposure to 16 $\mu$M ISO. (D) Terminal deoxynucleotidyl transferase dUTP nick end labeling assay after exposure to 16 $\mu$M ISO for 48 h (apoptotic bodies in green color) (scale bars, 50 $\mu$m). (E) A549 cells were treated with indicated concentrations of ISO for 24 h, and cell apoptosis was measured by Annexin V/PI staining. ISO, isorhamnetin; FITC, fluorescein isothiocyanate; PI, propidium iodide.

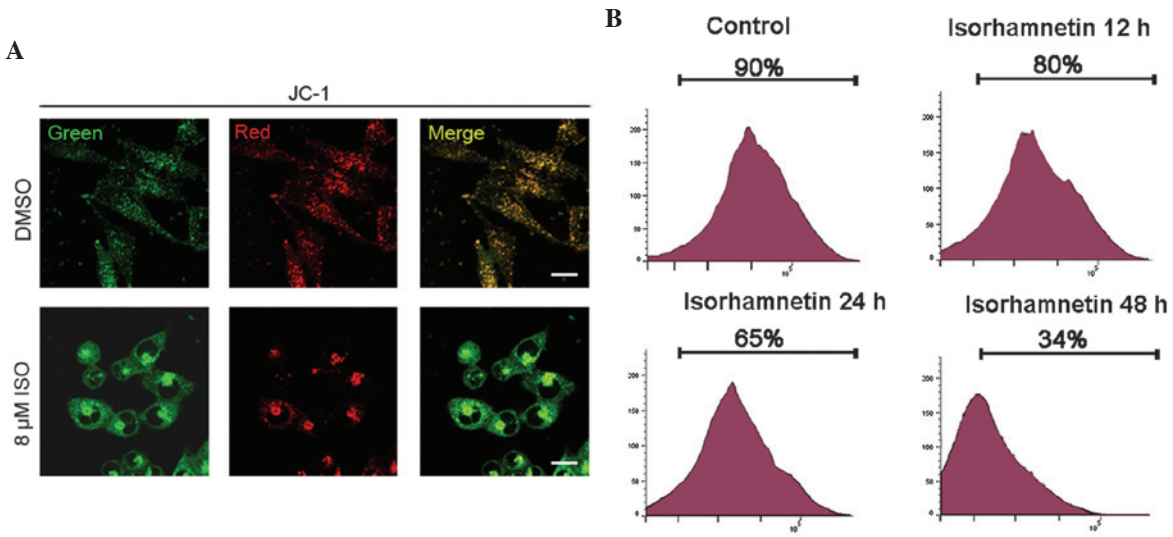


Figure 2. ISO induces apoptosis in A549 cells. (A) A549 cells were treated with indicated concentrations of ISO for 24 h, and mitochondrial membrane potential was detected using JC-1 staining method (scale bars, 10 $\mu$m). (B) Cells were treated with 16 $\mu$M ISO for the indicated times, harvested and stained with tetramethylrhodamine ethyl ester to determine mitochondrial membrane potential by flow cytometry. ISO, isorhamnetin; DMSO, dimethyl sulfoxide.

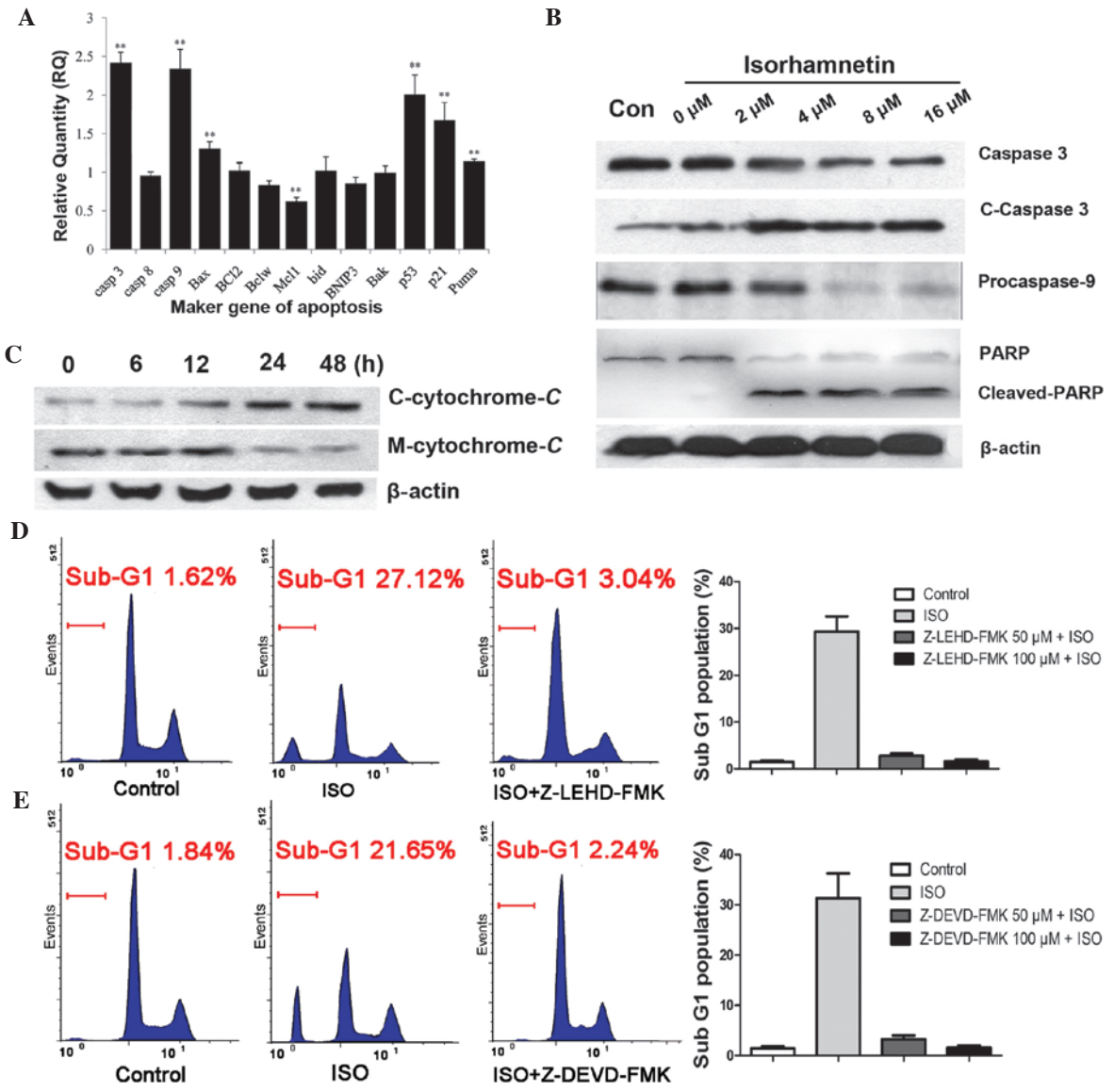


Figure 3. ISO induces mitochondria-dependent caspase activation (A) Treatment with 8 $\mu$M ISO for 12 h induced alterations in the mRNA expression of marker genes associated with apoptosis in A549 cells. (B) Cleaved-caspase-3, cleaved-PARP and pro-caspase-9 were detected after treatment with the indicated concentrations of ISO for 24 h. (C) A significant increase of cytochrome *C* release was detected at 12 h after 16-$\mu$M ISO treatment. (D and E) Caspase-9 inhibitor Z-LEHD-FMK or caspase-3/7 inhibitor Z-DEVD-FMK significantly blocked the ISO-induced sub-$G_1$ peaks. Cells were treated with 8 $\mu$M ISO for 48 h. Values are expressed the mean ± standard deviation (n=4). $^{**}$P<0.01. C-cytochrome *C*, cytosolic cytochrome *C*; M-cytochrome *C*, mitochondrial cytochrome *C*; ISO, isorhamnetin; casp, caspase; Bcl-2, B-cell lymphoma 2; Bax, Bcl-2-associated X protein; Bclw, Bcl-2-like protein 2; Mcl1, myeloid cell leukemia 1; bid, BH3 interacting-domain death agonist; BNIP3, Bcl-2/adenovirus E1B 19 kDa protein-interacting protein 3; Bak, Bcl-2 homologous antagonist/killer; Puma, p53-upregulated modulator of apoptosis; Con, control; PARP, poly(adenosine diphosphate ribose) polymerase.

the control cells to 80.6, 65.5, and 34.2% at 12, 24, and 48 h of ISO treatment, respectively (Fig. 2B).

Furthermore, the ISO-induced alterations in the mRNA expression of apoptosis marker genes in A549 cells were examined. RT-qPCR analysis showed a significant (P<0.01) upregulation in the expression of caspase-3 (9.6±0.53-fold), caspase-9 (9.4±0.65-fold), Bax (1.6±0.19-fold), p53 (5.89±0.21-fold), p21 (2.7±0.33-fold) and Puma (2.22±0.23-fold) at 12 h of treatment with 8 $\mu$M ISO (Fig. 3A). In addition, the protein expression of cleaved-caspase-3, cleaved-PARP and pro-caspase-9 were detected by western blotting. As shown in Fig. 3B, the expression levels of cleaved-caspase-3 and cleaved-PARP were significantly increased following ISO treatment in a dose-dependent manner, whereas the levels of pro-caspase-9 were obviously decreased, indicating that ISO treatment resulted in the activation of the caspase-dependent apoptotic pathway. As it is known that caspase activation involves changes in mitochondrial permeability and the release of cytochrome *C*, the levels of cytochrome *C* in the cytosolic fraction were then examined. As shown in Fig. 3C, a significant increase of released cytochrome *C* was detected at 12 h after treatment with 16 $\mu$M ISO. To further determine whether the ISO-induced apoptosis of NSCLC cells was caspase-mediated, A549 cells were incubated with caspase-9 inhibitor Z-LEHD-FMK or caspase-3/7 inhibitor Z-DEVD-FMK for 2 h followed by treatment of the cells with ISO for 48 h (Fig. 3D and E). These caspase inhibitors completely blocked the ISO-induced sub-G1 fractions in the cell cycle distribution. These results therefore suggested that ISO-induced apoptosis was mediated by mitochondria-dependent caspase activation.

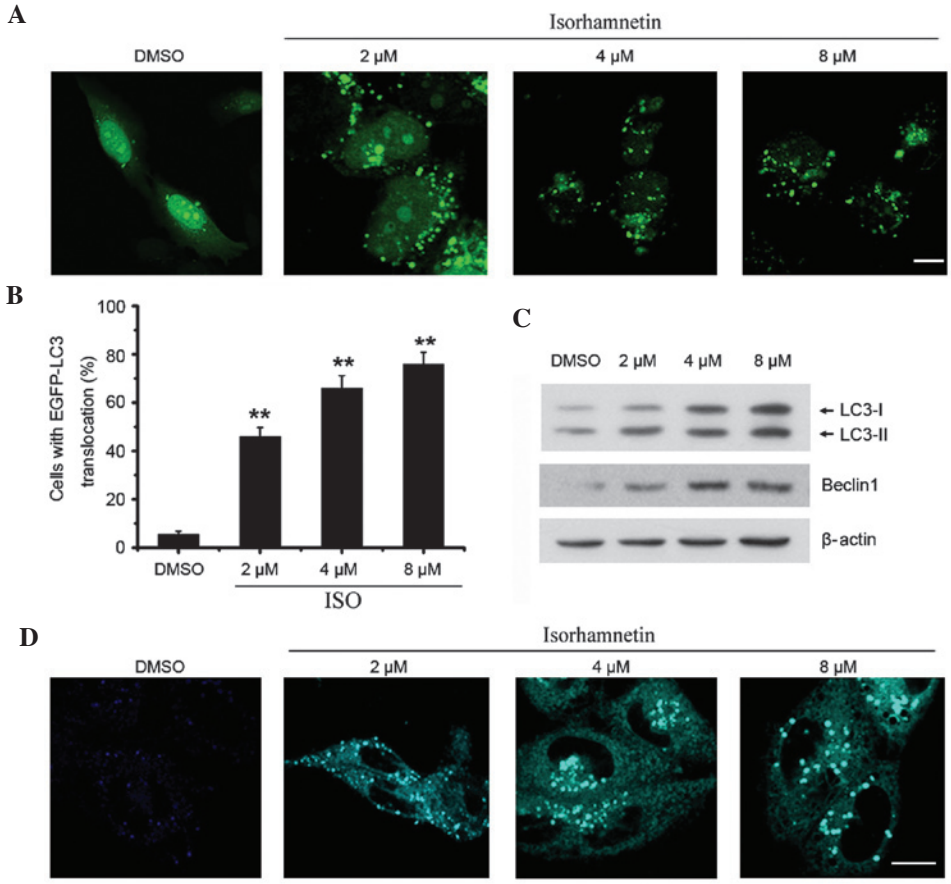


Figure 4. ISO induces autophagy in A549 cells. (A) pEGFP-LC3-transfected A549 cells were treated with different concentrations of ISO for 24 h and the GFP-LC3-II translocation to autophagosomes was observed using confocal microscopy (scale bar, 10 $\mu$m). (B) The percentages of cells with LC3 translocation, as indicated by formation of dots, were counted (n=250 cells/sample). Cells were treated wth various concentrations of ISO for 24 h. Values are expressed the mean ± standard deviation of three independent experiments ($^{**}$P<0.01). (C) A549 cells were treated with indicated concentrations of ISO for 24 h and endogenous LC3-II levels were detected by western blotting using LC3B antibody. (D) A549 cells were treated with indicated concentrations of ISO for 24 h and autophagy was detected by monodansylcadaverine staining (scale bar, 10 $\mu$m). EGFP, enhanced green fluorescence protein; ISO, isorhamnetin; DMSO, dimethyl sulfoxide; LC3, microtubule-associated protein 1 light chain 3.

*ISO induces autophagy in NSCLC cells*. Numerous chemotherapeutic agents designed to kill cancer cells are also known to induce autophagy (18). When autophagy is initiated, microtubule-associated protein 1 light chain 3 (LC3) is cut on the C-terminal to produce LC3-II protein. The resulting LC3-II is then preferentially translocated to the membranes of autophagosomes and shows a punctate staining pattern in the cytosol (33). In order to detect autophagy, EGFP-LC3 was overexpressed in A549 cells. As shown in Fig. 4A and B, the number of autophagosomes with a punctate staining pattern was significantly increased in ISO-treated cells compared with that in untreated cells. Accordingly, the protein levels of LC3-II were also significantly increased in A549 cells treated with ISO in a dose-dependent manner (Fig. 4C). Beclin1 has been shown to be the activator of the Class III phosphoinositide 3-kinase (PI3K) complex that has an important role in the regulation of autophagy induction (34). In the present study, it was found that the expression of Beclin1 was upregulated following ISO treatment (Fig. 4C).

To further confirm that ISO indeed induced autophagosome formation, an MDC staining assay was performed. Similar to the results of the EGFP-LC3-II translocation assay, ISO treatment also induced apparent accumulation of MDC in the cytoplasmic vacuoles compared to that in the control cells (Fig. 4D).

*Inhibition of autophagy enhances the growth inhibition and pro-apoptotic effect of ISO*. 3-MA is a PI3K inhibitor, which suppresses autophagy formation by blocking the activity of the the Class III PI3K complex at an early stage of autophagy (35,36). CQ inhibits autophagy by interfering with the fusion of autophagosomes and lysosomes at a late stage of autophagy (37,38). As shown in Fig. 5A, pre-treatment with 3-MA significantly inhibited the ISO-induced autophagosome formation in the A549 cells (Fig. 5A and B). By contrast, an increased amount of ISO-induced autophagosomes was accumulated in the A549 cells pre-treated with CQ compared with that in cells treated with ISO only (Fig. 5A and B). Next, the protein levels of endogenous LC3-II were detected. As expected, 3-MA pre-treatment significantly inhibited the formation of endogenous LC3-II protein in ISO-treated cells, compared to that in cells treated with ISO only. However, there was no obvious difference in endogenous LC3-II levels between cells treated with ISO only and those co-treated with CQ (Fig. 5C).

Next, the effect of autophagy inhibition on ISO-induced growth inhibition and apoptosis was investigated. An MTT assay showed that pre-treatment with 3-MA or CQ markedly enhanced the growth inhibition induced by ISO treatment (Fig. 5D). Consistent with the MTT assay, the number of

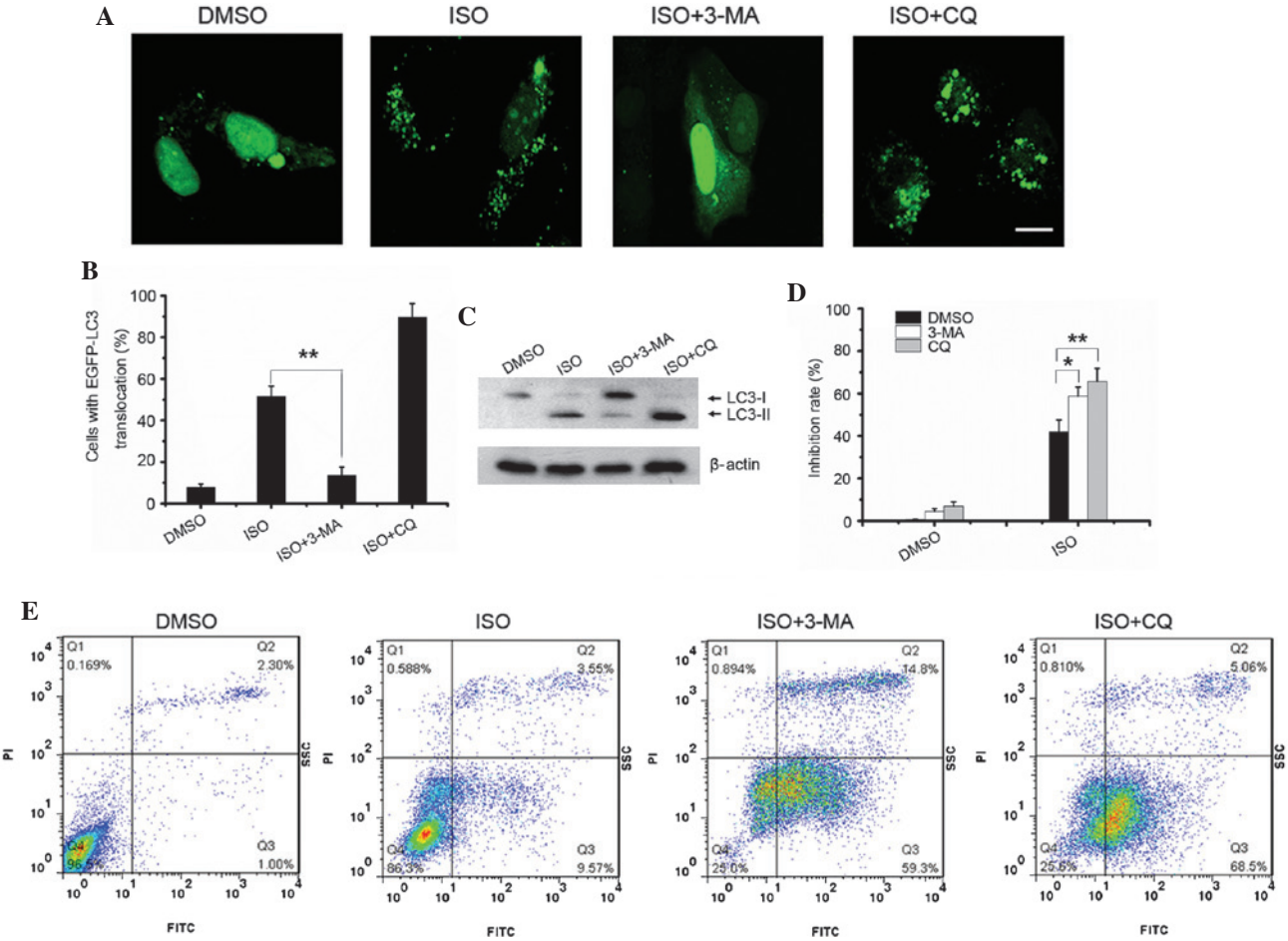


Figure 5. Inhibition of autophagy sensitizes A549 cells to ISO-induced growth inhibition and apoptosis. (A) pEGFP-LC3-transfected A549 cells were treated with 4 $\mu$M isorhamnetin alone or in combination with 10 mM 3-MA or 50 $\mu$M CQ for 24 h, and autophagy was observed using confocal microscopy (scale bar, 10 $\mu$m). (B) The percentages of cells with LC3 translocation as indicated by the formation of dots were counted (n=250 cells/sample). Values are expressed as the mean ± standard deviation of three independent experiments ($^{**}$P<0.01). (C) Endogenous LC3-II levels in cells with the same treatment as in A were detected by western blotting using the LC3B antibody. (D) A549 cells were treated as in C, and an MTT cell viability assay was conducted. Values are expressed as the mean ± standard deviation of three independent experiments ($^{*}$P<0.05; $^{**}$P<0.01). (E) A549 cells were treated as in C and apoptosis was detected using Annexin V/PI staining followed by flow cytometric analysis. ISO, isorhamnetin; DMSO, dimethyl sulfoxide; LC3, microtubule-associated protein 1 light chain 3; PI, propidium iodide; MA, methyladenine; EGFP, enhanced fluorescence protein; CQ, hydroxychloroquine; FITC, fluorescein isothiocyanate.

ISO-induced apoptotic cells was also markedly increased in the cells pre-treated with 3-MA and CQ compared with that in cells treated with ISO only (Fig. 5E). Collectively, these results suggested that inhibition of autophagy sensitized the A549 cells to ISO-induced growth inhibition and apoptosis.

*Inhibitors of autophagy significantly enhance the inhibitory effect of ISO on mouse xenograft tumors*. Confirmed by the marked anti-proliferative and apoptosis-inducing activities observed in cell culture experiments, the present study examined the anti-tumor activity of ISO *in vivo*. BALB/c nu/nu mice bearing A549 NSCLC xenografts were given a daily intraperitoneal injection of ISO. In a preliminary study, ISO showed an *in vivo* anti-tumor activity at 0.5 mg/kg/day, and this dose was therefore used in the present study. The growth of xenografts was monitored every three days over two weeks. Side effects, including body weight loss, mortality and lethargy were not observed in mice treated by ISO for two weeks. The final tumor size was markedly lower in the majority of the 0.5 mg/kg ISO-treated mice compared with that in the control group. Of note, the tumor size was significantly lower in the group co-injected with 3-MA (22.4 mg/kg) or CQ (10 mg/kg) (Fig. 6A), compared with that in the mice injected with ISO only. The tumor weight was 2.11±0.35 g in the control mice, 0.91±0.27 g in ISO-treated mice, 0.42±0.12 g in ISO and 3-MA co-injected mice and 0.58±0.16 in ISO and CQ co-injected mice, respectively (Fig. 6B). The results therefore indicated that autophagy inhibition markedly promoted the inhibitory effect of ISO on the NSCLC xenograft tumors.

*Suppression of autophagy decreases ISO-induced growth suppression and enhances apoptosis of NSCLC in vivo*. To assess apoptosis in the experimental groups, TUNEL-positive cells were detected in the tumor tissue. Quantitative evaluation showed that the apoptotic index was 7±3% in the control tumors, while it was 33±5% in the ISO-treated tumors. As expected, the apoptotic index was increased to 65±8% in the ISO and 3-MA co-treated tumors, and 60±9% in the ISO and CQ co-treated tumors (Fig. 6C and D). In addition, the levels of cleaved caspase-3 showed a similar trend to that of the apoptotic rate in the different experimental groups (Fig. 6C and D). The proliferative indices in the groups were also assessed; as

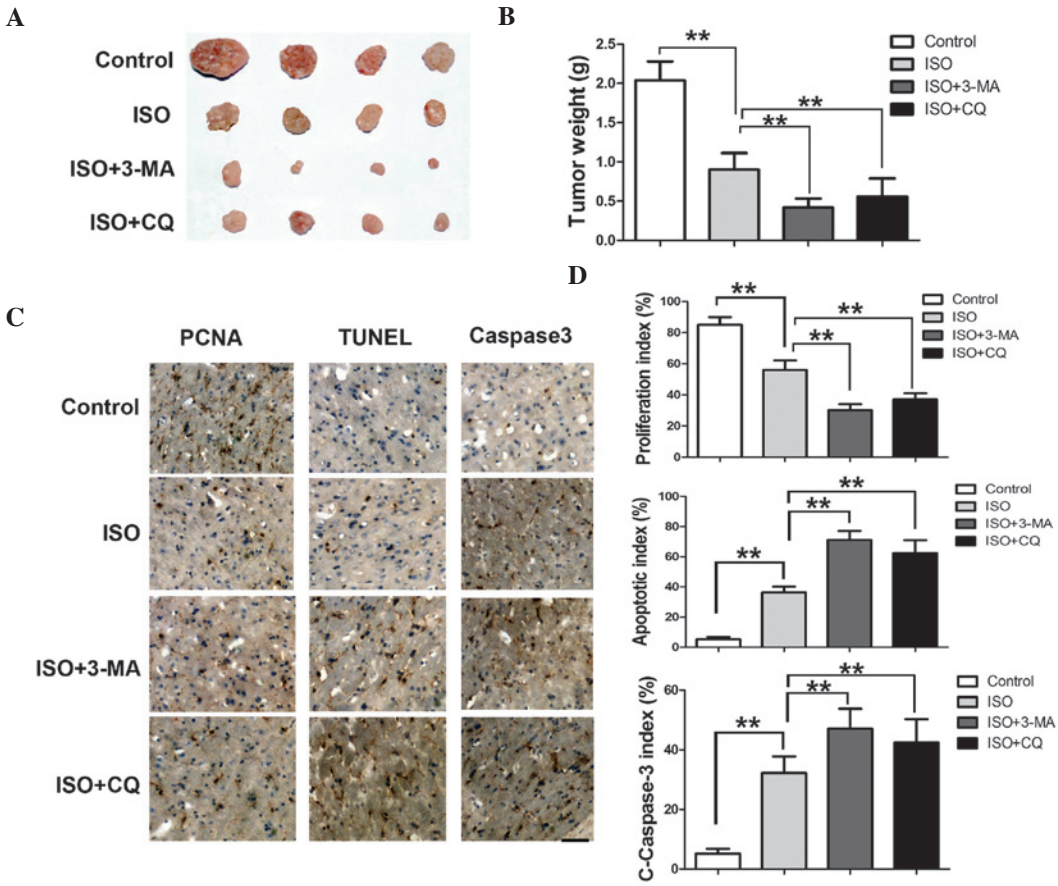


Figure 6. Autophagy inhibition enhances the growth inhibitory effect of ISO on A549 xenograft tumors. (A) Images of harvested tumors at the end of the experiment. (B) Weights of tumors from the mice after two weeks of indicated treatments. (C) Representative immunohistochemical staining for PCNA and c-caspase-3 as well as TUNEL staining (scale bar, 50 $\mu$m). (D) The proliferative and apoptotic index was calculated by the ratio of positive cells vs. total cells. Values are expressed as the mean ± standard deviation (n=6). $^{**}$P<0.01. PCNA, Proliferating cell nuclear antigen; TUNEL, Terminal deoxynucleotidyl transferase dUTP nick end labeling; CQ, hydroxychloroquine; ISO, isorhamnetin; MA, methyladenine; C-caspase, cleaved caspase.

shown in Fig. 6D, in the control group, the proliferative index was 81±7%, whereas in all treatment groups, the proliferation was markedly decreased to 51±4% in the ISO-treated group, 23±5% in the ISO- and 3-MA-treated group and 32±4% in the ISO and CQ co-injected group. These results therefore supported that caspase-mediated apoptosis is a key contributor to tumor growth suppression and that suppression of autophagy markedly promoted the inhibitory effect of ISO on NSCLC.

## Discussion

ISO, an immediate 3'-O-methylated metabolite of quercetin, has been studied in recent years for its marked anti-cancer activity in several human cancer types (6-8). However, to date, the anti-cancer effects of ISO have not been investigated in lung cancer. In the present study, the anti-proliferative and pro-apoptotic effects of ISO on human NSCLC cells were investigated *in vitro* and *in vivo*. The results showed that ISO efficiently inhibited the proliferation and induced apoptosis of NSCLS cells in a time- and dose-dependent manner, indicating that ISO may be a potential candidate for a novel anti-lung cancer drug.

Numerous chemotherapeutic drugs designed to kill cancer, most likely by inducing apoptosis, including fluorouracil, arsenic trioxide, tamoxifen, paclitaxel, adriamycin and cisplatin, have been shown to also induce autophagy (39,40). The present study found that ISO treatment of A549 cells resulted in the upregulated expression of endogenous LC3-II and Beclin1, the translocation to autophagosomes of GFP-LC3-II, and the accumulation of MDC in cytoplasmic vacuoles, suggesting that ISO also induced autophagy in lung cancer cells.

The *in vitro* and *in vivo* experiments of the present study as described above significantly enhanced the mechanistic understanding of the signaling events involved in the induction of apoptosis in lung cancer cells by ISO as well as their relevance to its *in vivo* tumor-inhibitory efficacy. Mechanistically, the *in vitro* results suggested that the induction of apoptosis by ISO proceeds through a mitochondrial pathway. This was indicated by loss of the transmembrane potential as cytochrome *C* was released into cytosolic fraction, decreased pro-caspase-9 levels (through cleavage), increased cleaved caspase-3 and PARP levels as well as DNA fragmentation, TUNEL positivity and sub-G1 apoptotic bodies. The critical role of the mitochondria/cytochrome *C*/caspase-9 cascade was supported by the complete blockage of apoptosis by the caspase-9 inhibitor Z-LEHD-FMK and caspase-3 inhibitor Z-DEVD-FMK. The detailed mechanisms of how ISO affects the mitochondria to initiate apoptosis signaling as well as a possible involvement of mitogen-associated protein kinase (MAPK) pathways

(extracellular signal-regulated kimase, c-Jun N-terminal kinase and p38MAPK) pathways or the PI3K-AKT survival pathway require further investigation.

Autophagy has major protective roles in maintaining the homeostasis in the cells by clearing damaged organelles, such as mitochondria, and toxic proteins (40,41). However, the functions and mechanisms of drug-induced autophagy in cancer cells have remained to be fully elucidated (42,43). Most studies indicated that drug-induced autophagy can be divided into two types: Pro-survival autophagy and pro-death autophagy. Pro-survival autophagy induced by chemotherapeutic drugs was found to reduce the anti-tumor effects of the drugs, which indicated the presence of a cross-talk between apoptotic signaling and autophagy (44-46). The present study investigated the contributions of autophagy to ISO-induced apoptosis of lung cancer cells, and the results showed that ISO was able to induce autophagy. Pre-treatment with autophagy inhibitors 3-MA and CQ efficiently suppressed ISO-induced autophagy and enhanced ISO-induced growth inhibition as well as apoptosis in lung cancer cells. The results therefore indicated that ISO induced a pro-survival-type autophagy, and that co-treatment with autophagy inhibitors can be used to improve the therapeutic effects of ISO in lung cancer. The analyses of the mouse xenograft tumors showed a decreased PCNA index (~20% reduction), as well as >four-fold increases of TUNEL- and cleaved-caspase-3-positive tumor cells when the animals were co-treated with 3-MA or CQ compared with those following treatment with ISO only. This demonstrated that autophagy inhibition markedly promoted the suppressive effect of ISO on the growth of NSCLC xenograft tumors.

In conclusion, the present study demonstrated that ISO may serve as an anti-tumor agent to significantly suppress the cell viability and promote apoptosis of lung cancer cells. In addition, ISO treatment also induced a pro-survival-type autophagy and inhibition of this type of autophagy may enhance ISO-induced growth inhibition and apoptosis in lung cancer cells. Thus, the present study suggested the combined treatment with ISO and inhibitors of autophagy as an efficient strategy for anti-lung cancer therapy.

## Acknowledgements

The authors would like to thank Mr. Wugen Zhan for the assistance with the flow cytometric analysis, and Mr. Yu Bing for the assistance with the microscopic analysis (both Division of Life and Health Sciences, Shenzhen Graduate School of Tsighua University, Shenzhen, China). The present study was supported by the Guangdong Natural Science Foundation (no. 2014A030313758), a Doctoral Fund of the Ministry of Education of China (no. 20120002120020) and the Science, Technology & Innovation Commission of Shenzhen Municipality (no. JCYJ20140417115840285).

## References

1. Molina JR, Yang P, Cassivi SD, Schild SE and Adjei AA: Non-small cell lung cancer: Epidemiology, risk factors, treatment, and survivorship. Mayo Clin Proc 83: p. 584-594, 2008.
2. Tada H, Tsuchiya R, Ichinose Y, Koike T, Nishizawa N, Nagai K and Kato H: A randomized trial comparing adjuvant chemotherapy versus surgery alone for completely resected pN2 non-small cell lung cancer (JCOG9304). Lung Cancer 43: 167-173, 2004.
3. Asano N, Kuno T, Hirose Y, Yamada Y, Yoshida K, Tomita H, Nakamura Y and Mori H: Preventive effects of a flavonoid myricitrin on the formation of azoxymethane-induced premalignant lesions in colons of rats. Asian Pac J Cancer Prev 8: 73-76, 2007.
4. Khacha-ananda S, Tragoolpua K, Chantawannakul P and Tragoolpua Y: Antioxidant and anti-cancer cell proliferation activity of propolis extracts from two extraction methods. Asian Pac J Cancer Prev 14: 6991-6995, 2013.
5. Manu KA, Shanmugam MK, Ramachandran L, *et al*: Isorhamnetin augments the anti-tumor effect of capeciatbine through the negative regulation of NF-κB signaling cascade in gastric cancer. Cancer Lett 363: 28-36, 2015.
6. Saud SM, Young MR, Jones-Hall YL, Ileva L, Evbuomwan MO, Wise J, Colburn NH, Kim YS and Bobe G: Chemopreventive activity of plant flavonoid isorhamnetin in colorectal cancer is mediated by oncogenic Src and beta-catenin. Cancer Res 73: 5473-84, 2013.
7. Li C, Yang X, Chen C, Cai S and Hu J: Isorhamnetin suppresses colon cancer cell growth through the PI3K-Akt-mTOR pathway. Mol Med Rep 9: 935-940, 2014.
8. Ramachandran L, Manu KA, Shanmugam MK, Li F, Siveen KS, Vali S, Kapoor S, Abbasi T, Surana R, Smoot DT, *et al*: Isorhamnetin inhibits proliferation and invasion and induces apoptosis through the modulation of peroxisome proliferator-activated receptor gamma activation pathway in gastric cancer. J Biol Chem 287: 38028-38040, 2012.
9. Fulda S and Debatin KM: Debatin, extrinsic versus intrinsic apoptosis pathways in anticancer chemotherapy. Oncogene 25: 4798-4811, 2006.
10. Zhao J, Wang SZ, Tang XF, Liu N, Zhao D and Mao ZY: Analysis of thermochemotherapy-induced apoptosis and the protein expressions of Bcl-2 and Bax in maxillofacial squamous cell carcinomas. Med Oncol, 28 (Suppl 1): S354-S359, 2011.
11. Kim R: Recent advances in understanding the cell death pathways activated by anticancer therapy. Cancer 103: 1551-1560, 2005.
12. Fang K, Chen Z, Liu M, Peng J and Wu P: Apoptosis and calcification of vascular endothelial cell under hyperhomocysteinemia. Med Oncol 32: 403, 2015.
13. Choi KS: Autophagy and cancer. Exp Mol Med 44: 109-120, 2012.
14. Liu D, Yang Y, Liu Q and Wang J: Inhibition of autophagy by 3-MA potentiates cisplatin-induced apoptosis in esophageal squamous cell carcinoma cells. Med Oncol 28: 105-111, 2011.
15. Mathew R, Karantza-Wadsworth V and White E: Role of autophagy in cancer. Nat Rev Cancer 7: 961-967, 2007.
16. Mathew R and White E: Why sick cells produce tumors: The protective role of autophagy. Autophagy 3: 502-505, 2007.
17. White E: Deconvoluting the context-dependent role for autophagy in cancer. Nat Rev Cancer, 12: 401-410, 2012.
18. Mah LY and Ryan KM: Autophagy and cancer. Cold Spring Harb Perspect Biol 4: a008821, 2012.
19. Karantza-Wadsworth V and White E: Role of autophagy in breast cancer. Autophagy, 3: 610-613, 2007.
20. Maycotte P, Aryal S, Cummings CT, Thorburn J, Morgan MJ and Thorburn A: Chloroquine sensitizes breast cancer cells to chemotherapy independent of autophagy. Autophagy 8: 200-212, 2012.
21. Maclean KH, Dorsey FC, Cleveland JL and Kastan MB: Targeting lysosomal degradation induces p53-dependent cell death and prevents cancer in mouse models of lymphomagenesis. J Clin Invest, 118: 79-88, 2008.
22. Zhang X, Dong Y, Zeng X, Liang X, Li X, Tao W, Chen H, Jiang Y, Mei L and Feng SS: The effect of autophagy inhibitors on drug delivery using biodegradable polymer nanoparticles in cancer treatment. Biomaterials 35: 1932-1943, 2014.
23. Gibson UE, Heid CA and Williams PM. A novel method for real time quantitative RT-PCR. Genome Res 6: 995-1001, 1996.
24. Høyer-Hansen M, Bastholm L, Szyniarowski P, Campanella M, Szabadkai G, Farkas T, Bianchi K, Fehrenbacher N, Elling F, Rizzuto R, *et al*: Control of macroautophagy by calcium, calmodulin-dependent kinase kinase-beta, and Bcl-2. Mol Cell 25: 193-205, 2013.
25. Abnosi MH, Solemani Mehranjani M, Momeni HR, Mahdiyeh Najafabadi M, Barati M and Shojafar E: The induction of apoptosis and autophagy in rat bone marrow mesenchymal stem cells following *in vitro* treatment with p-nonylphenol. IJST A3: 239-244, 2012.
26. Estavillo GM, Verhertbruggen Y, Scheller HV, *et al*: Isolation of the plant cytosolic fraction for proteomic analysis. Methods Mol Biol 1072: 453-467, 2014.

27. Kalani K, Agarwal J, Alam S, Khan F, Pal A and Srivastava SK: In silico and in vivo anti-malarial studies of 18β glycyrrhetinic acid from *Glycyrrhiza glabra*. PLoS One 8: e74761, 2013.
28. Hasenjäger A, Gillissen B, Müller A, Normand G, Hemmati PG, Schuler M, Dörken B and Daniel PT: Smac induces cytochrome *c* release and apoptosis independently from Bax/Bcl-x(L) in a strictly caspase-3-dependent manner in human carcinoma cells. Oncogene 23: 4523-4535, 2004.
29. Suzuki S, Higuchi M, Proske RJ, Oridate N, Hong WK and Lotan R: Implication of mitochondria-derived reactive oxygen species, cytochrome C and caspase-3 in *N*-(4-hydroxyphenyl) retinamide-induced apoptosis in cervical carcinoma cells. Oncogene 18: 6380-6387, 1999.
30. Cuvillier O, Nava VE, Murthy SK, Edsall LC, Levade T, Milstien S and Spiegel S: Sphingosine generation, cytochrome c release, and activation of caspase-7 in doxorubicin-induced apoptosis of MCF7 breast adenocarcinoma cells. Cell Death Differ 8: 162-171, 2001.
31. Zhang W, Wang Z and Chen T: Curcumol induces apoptosis via caspases-independent mitochondrial pathway in human lung adenocarcinoma ASTC-a-1 cells. Med Oncol, 28: 307-314, 2011.
32. Li XY, Lin YC, Huang WL, Lin W, Wang HB, Lin WZ and Lin SL: Zoledronic acid inhibits human nasopharyngeal carcinoma cell proliferation by activating mitochondrial apoptotic pathway. Med Oncol 29: 3374-3380, 2012.
33. Mizushima N, Yoshimori T and Levine B: Methods in mammalian autophagy research. Cell 140: 313-326, 2010.
34. Kim MS, Jeong EG, Ahn CH, Kim SS, Lee SH and Yoo NJ: Frameshift mutation of UVRAG, an autophagy-related gene, in gastric carcinomas with microsatellite instability. Hum Pathol 39: 1059-1063, 2008.
35. Hoare M, Young AR and Narita M: Autophagy in cancer: Having your cake and eating it. Semin Cancer Biol 21: 397-404, 2011.
36. Liu F, Liu D, Yang Y and Zhao S: Effect of autophagy inhibition on chemotherapy-induced apoptosis in A549 lung cancer cells. Oncol Lett 5: 1261-1265, 2013.
37. Pellegrini P, Strambi A, Zipoli C, Hägg-Olofsson M, Buoncervello M, Linder S and De Milito A: Acidic extracellular pH neutralizes the autophagy-inhibiting activity of chloroquine: Implications for cancer therapies. Autophagy 10: 562-571, 2014.
38. Zou Y, Ling YH, Sironi J, Schwartz EL, Perez-Soler R and Piperdi B: The autophagy inhibitor chloroquine overcomes the innate resistance of wild-type EGFR non-small-cell lung cancer cells to erlotinib. J Thorac Oncol 8: 693-702, 2013.
39. Lozy F and Karantza V: Autophagy and cancer cell metabolism. Semin Cell Dev Biol 23: 395-401, 2012.
40. Giuliani CM and Dass CR: Autophagy and cancer: Taking the 'toxic' out of cytotoxics. J Pharm Pharmacol 65: 777-789, 2013.
41. Gewirtz DA: Autophagy and senescence in cancer therapy. J Cell Physiol 229: 6-9, 2014.
42. He W, Ma X, Yang X, Zhao Y, Qiu J and Hang H: A role for the arginine methylation of Rad9 in checkpoint control and cellular sensitivity to DNA damage. Nucleic Acids Res 39: 4719-4727, 2011.
43. He W, Zhao Y, Zhang C, An L, Hu Z, Liu Y, Han L, Bi L, Xie Z, Xue P, *et al*: Rad9 plays an important role in DNA mismatch repair through physical interaction with MLH1. Nucleic Acids Res 36: 6406-6417, 2008.
44. Eng CH and Abraham RT: The autophagy conundrum in cancer: Influence of tumorigenic metabolic reprogramming. Oncogene 30: 4687-4696, 2011.
45. Jain K, Paranandi KS, Sridharan S and Basu A: Autophagy in breast cancer and its implications for therapy. Am J Cancer Res 3: 251-265, 2013.
46. Lorin S, Hamaï A, Mehrpour M and Codogno P: Autophagy regulation and its role in cancer. Semin Cancer Biol 23: 361-379, 2013.